

LA-UR-10-03279

Approved for public release;  
distribution is unlimited.

<i>Title:</i>	Los Alamos National Laboratory Results for the 2009 SILENE Criticality Accident Dosimetry Exercise: Final Report
<i>Author(s):</i>	Milan S. Gadd, RP-2 Victoria M. Homan, RP-2
<i>Intended for:</i>	DOE Exercise Coordinator (LLNL) RP-2 File



Los Alamos National Laboratory, an affirmative action/equal opportunity employer, is operated by the Los Alamos National Security, LLC for the National Nuclear Security Administration of the U.S. Department of Energy under contract DE-AC52-06NA25396. By acceptance of this article, the publisher recognizes that the U.S. Government retains a nonexclusive, royalty-free license to publish or reproduce the published form of this contribution, or to allow others to do so, for U.S. Government purposes. Los Alamos National Laboratory requests that the publisher identify this article as work performed under the auspices of the U.S. Department of Energy. Los Alamos National Laboratory strongly supports academic freedom and a researcher's right to publish; as an institution, however, the Laboratory does not endorse the viewpoint of a publication or guarantee its technical correctness.

# Los Alamos National Laboratory Results for the 2009 SILENE Criticality Accident Dosimetry Exercise: Final Report

Milan S. Gadd and Victoria M. Homan  
Health Physics Measurements Group (RP-2)  
Health Physics Analysis Laboratory (HPAL) Team

## Introduction

October 9-20, 2009, Los Alamos National Laboratory (LANL) participated in a criticality accident dosimetry exercise at CEA Valduc, France. The exercise was funded by the U.S. Department of Energy Nuclear Criticality Safety Program and coordinated through Lawrence Livermore National Laboratory (LLNL). Other facilities represented included LLNL, Pacific Northwest National Laboratory, Y-12, Savannah River Site, and Oak Ridge National Laboratory.

The exercise was conducted using the SILENE reactor, which is a liquid solution assembly, operated in the pulse mode (Asselineau, et. al., 2004). Three exposures were performed consisting of a pulse with the assembly shielded by 10 cm lead, an unshielded (bare) low-power pulse, and a bare high-power pulse. Participants were free to select the placement of their dosimetry materials according to the radial distance from the center axis of the assembly, orientation to the assembly, and whether or not they were placed on a phantom.

The goals for LANLs participation were to: 1) test and validate the procedures and algorithms used to determine doses resulting from a criticality accident; 2) compare the response of the new Personnel Neutron Dosimeters (PNDs), manufactured by Shieldwerx<sup>1</sup>, to those previously used at LANL; and 3) re-evaluate the use of operational field equipment for the measurement of accident dosimeter materials. The second goal stems from the observed degradation of the indium foils in some older PNDs.

## Methods

The LANL PND contains four activation elements consisting of bare and cadmium shielded indium foils, a cadmium covered copper foil, and a bare sulfur tablet. A line drawing of the PND is shown in Figure 1 and the reactions of interest are summarized in Table 1. Detailed information on the PND elements can be found in the Los Alamos Personnel and Area Criticality Dosimeter Systems technical basis document (LANL, 2006). Personnel PNDs are typically issued to an individual and not exchanged on any schedule. In 2008 it was decided to exchange all issued PNDs with new ones. This was due to degradation of the indium foils observed in some old PNDs and the institution of a system to assign specific PNDs to individuals. The fundamental design of the PND was not changed but they were obtained from a different supplier.

For each exposure, new and old PNDs were paired along with a LANL 8823 Whole Body TLD (Hoffman and Mallet, 1999). The TLD is used to measure the photon dose,  $D_\gamma$ , as well as provide an additional measure of the neutron dose ( $D_n$ ). The TLD neutron dose is based on the Albedo/Anti-Albedo responses of four TLD elements. An algorithm calculates the dose based on the relative response as compared to a calibration curve for bare and polyethylene moderated <sup>252</sup>Cf spectra. The dosimeter placements are summarized in Table 2.

Following the exposures, the activation elements were analyzed using the methods described by Devine, et. al. (2004). Counts were performed using an Eberline E-600 Digital Survey Meter<sup>2</sup> with either a 2x2 NaI(Tl) SPA-3

---

<sup>1</sup> Shieldwerx™, 4135 Jackie Rd SE #108, Rio Rancho, New Mexico 87124

<sup>2</sup> Thermo Fisher Scientific, Inc. 27 Forge Parkway, Franklin, MA 02038

detector or a HP-360 "Pancake" GM probe attached. For use with the SPA-3 detector the E-600 was configured for two channels. The first channel was optimized for counting energies similar to  $^{60}\text{Co}$  (1.17 and 1.33 MeV) and the second for  $^{137}\text{Cs}$  energies (0.662 MeV). The beta probe (HP-360) was calibrated using  $^{90}\text{Sr}/^{90}\text{Y}$  and  $^{36}\text{Cl}$  sources. To reduce the background and potential interference from nearby samples, counts were performed inside of shields constructed of 5x10x20 cm lead bricks. Additionally, selected foils were analyzed using the high-purity germanium (HPGe) detector brought by LLNL and the results compared to those obtained using the E-600 and SPA-3 detector.

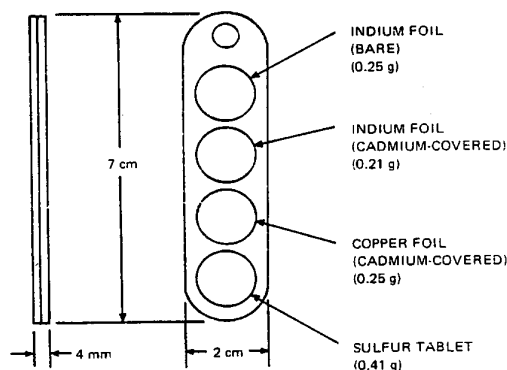


**Figure 1.** LANL Personnel Neutron Dosimetry (PND) packet.

**Table 1.** LANL PND Elements and Reactions

Neutron Energy	Reaction	Half Life	PND Element	Analysis
Thermal (<0.6 eV)	$^{115}\text{In}(n,\gamma)^{116\text{m}}\text{In}$	54 min.	Bare In Foil	1.293 MeV Gamma
1.2-20 MeV	$^{115}\text{In}(n,n')^{115\text{m}}\text{In}$	4.5 h	Cd Covered In Foil	0.831 MeV Beta
0.6 eV – 20 MeV	$^{63}\text{Cu}(n,\gamma)^{64}\text{Cu}$	12.8 h	Cd Covered Cu Foil	0.511 MeV Gamma
3.3 – 20 MeV	$^{32}\text{S}(n,p)^{32}\text{P}$	14.3 d	Sulfur Tablet	1.71 MeV Beta

**Table 2.** Dosimeter Placement

Run	Location Description	# Dosimeters
1 – Pb Shielded Pulse	2 m Phantom-Front	2 New PND 2 Old PND 2 TLD
	4 m Phantom-Front	3 New PND 3 Old PND 3 TLD
2 – Bare Low-Power Pulse	2 m Phantom-Front	3 New PND 3 Old PND 3 TLD
	2 m Phantom-Back	3 New PND 3 Old PND 3 TLD
3 – Bare High-Power Pulse	6 m Phantom-Front	3 New PND 3 Old PND 3 TLD
	6 m Free-in-Air	3 New PND 3 Old PND 3 TLD

All of the indium foils were counted the same day for  $^{116m}\text{In}$ . All other measurements were performed the next day. The  $^{115m}\text{In}$  activity was measured by counting of the 831 keV beta emission. Although the yield for the  $^{115m}\text{In}$  336 keV photon is greater than that for the beta, the beta detection efficiency is greater and the background is less susceptible to interference from other photon emitters. The copper foils were counted with 1 cm of polymethyl methacrylate, PMMA (e.g. Plexiglas™) placed between the foil and the SPA-3 detector to ensure the total annihilation of the  $^{64}\text{Cu}$  positron. The sulfur tablets were counted whole using the HP-360 probe and were also brought back to LANL, crushed to a powder, and counted using a gas-flow proportional counter. If there was an apparent loss of material, the elements were weighed and the actual masses used in the calculations. Otherwise, the average mass of the element was used. The actual crushed mass of the sulfur tablets were used in all calculations.

Calculation of the neutron fluence was performed using spectrum specific cross sections for the indium and sulfur elements (Devine, 2004) assuming threshold energies of 1.2 and 3.3 MeV, respectively. The spectra used in the calculations were those found in IAEA, 2001. For the copper foils, the effective cross section was adjusted until the relative proportions of the fluences in each energy region was similar to that found for the known spectrum. Spectrum specific fluence-to-dose conversion factors for the heavy particle recoil dose,  $\text{DCF}_{\text{HP}}$ , and  $\text{H}(n, \gamma)\text{D}$  reaction dose,  $(\text{DCF}_{n, \gamma})$ , were also calculated for each energy region. A summary of the factors used are given in Table 3.

Additional measurements were performed on phantoms filled with a  $2 \text{ g L}^{-1}$  NaCl solution. The phantoms simulate the human torso, having an approximately 25 cm x 40 cm oval cross section and a height of approximately 80 cm. This solution simulates the sodium concentration in the human body. These measurements were done to test the use of field survey equipment to screen potentially exposed workers.

**Table 3.** Effective cross sections and fluence to dose conversion factors.

Energy Region	Factor	Bare SILENE	Pb Shielded SILENE
Thermal (<0.6 eV)	$\text{In}(n, \gamma) \sigma_{\text{eff}}(\text{b})$	162.3	162.3
	$\text{DCF}_{\text{HP}} (\text{pGy cm}^2)$	0.58	0.58
	$\text{DCF}_{n, \gamma} (\text{pGy cm}^2)$	3.9	3.9
0.6 eV – 1.2 MeV	$\text{Cu}(n, \gamma) \sigma_{\text{eff}}(\text{b})$	0.37	0.26
	$\text{DCF}_{\text{HP}} (\text{pGy cm}^2)$	3.86	6.95
	$\text{DCF}_{n, \gamma} (\text{pGy cm}^2)$	2.94	2.56
1.2 – 3.3 MeV	$\text{In}(n, n') \sigma_{\text{eff}}(\text{b})$	0.306	0.285
	$\text{DCF}_{\text{HP}} (\text{pGy cm}^2)$	35.1	33.4
	$\text{DCF}_{n, \gamma} (\text{pGy cm}^2)$	1.37	1.41
>3.3 MeV	$\text{S}(n, \text{p}) \sigma_{\text{eff}}(\text{b})$	0.347	0.427
	$\text{DCF}_{\text{nHP}} (\text{pGy cm}^2)$	53.5	52.0
	$\text{DCF}_{n, \gamma} (\text{pGy cm}^2)$	1.23	1.07

## Results

An initial discovery following the first exposure run was that the new PND packets were very difficult to open due to the malleability of the new plastic and the adhesive used to seal the halves together. In addition some of the old PND casings were so brittle that they shattered instead of cleanly separating. Several packets, old and new, were damaged to the extent that all of the elements could not be retrieved for analysis. For the new packets it was found to be easier to cut a window in the top to access the elements.

There was no statistically significant difference in the induced specific activity for each of the elements between the old and new PNDs. Therefore, the results for the old and new PNDs at each run and location were averaged for use in calculating the neutron fluence and dose. There does appear to be a slightly greater variability in the indium foil results for the old PNDs, likely due to more variation in the foil masses.

There was no significant difference in the  $^{116m}\text{In}$  results between our measurements performed using the SPA-3 probe and LLNLs HPGe detector with an average ratio of the LANL to LLNL results of  $1.2 \pm 0.3$ . However, the  $^{115m}\text{In}$  activities based on the HP-360 beta measurements were an average of  $11.7 \pm 2.5$  times greater than those derived from the HPGe gamma measurements. The reason for this discrepancy has not been determined; however, it was concluded that the HPGe measurements more accurately represent the true activity. Therefore, all HP-360  $^{115m}\text{In}$  results were divided by 11.7 for use in the final fluence and dose calculations.

Initially the  $^{64}\text{Cu}$  activities measured using the SPA-3 were a factor of six or more greater than those measured by LLNLs HPGe. This was later determined to result from the use of the  $^{137}\text{Cs}$  662 keV photon set channel parameters on the E-600 and to determine the efficiency for SPA-3 probe. When the detector was re-calibrated using a  $^{22}\text{Na}$  source (511 keV), comparison of the results was more favorable with an average ratio of LANL to LLNL results of  $1.5 \pm 0.4$ . However, the LANL results were consistently greater than those measured by LLNL. This may be due to the foils being counted on the HPGe without any intervening material. The  $^{64}\text{Cu}$  using the 511 keV photon results from annihilation of the 653 keV positron. Therefore, it is important to ensure there is complete annihilation of the positron or the activity will be underestimated. The LANL procedure calls for the introduction of 1 cm of PMMA between the foil and the detector to ensure complete annihilation of the positron.

Comparisons of the  $^{32}\text{P}$  beta results measured at Valduc using the HP-360 GM probe and at LANL using a gas flow proportional counter (GFPC) were not favorable. The ratio of GFPC to GM results ranged from 1.07 to 17.0 with a mean of  $9.8 \pm 0.9$ . The reason for this discrepancy has not been determined at this time. There is no apparent correlation with the time between exposure and measurement, counting uncertainty, net GM count rate, or measured specific activity.

Appendix A contains a summary of the average specific activity induced in the PND elements for each exposure run. The calculated neutron fluences and doses can be found in Table 4.

The 8823 Whole Body TLD badges were processed using the standard algorithm with no corrections for supralinearity applied. Due to the high delivered doses it was necessary to install filters in the TLD readers in order to ensure proper readout of the results. In two cases filters were not used and there was incomplete collection of the luminescence resulting in an underestimate of the neutron dose<sup>3</sup>. The results contained Table 4 represent the average of the results for the badges exposed at each location. For all of the runs and positions, the neutron dose estimated from the 8823 badges are much greater than those calculated based on the PNDs. This indicates that the 8823 Whole Body TLD results may not give an accurate representation of the dose received by an individual in a criticality accident. Also, it should be noted that activation of the 8823 badge components may have resulted in additional dose to the elements after the exposure had ended. This may result in an over estimate of the photon dose.

Two sets of measurements were performed on the sodium phantoms. The first phantom was exposed during the first exposure run and was placed at 4 m. The second phantom was exposed at 6 m during the third run. Measurements were performed using the SPA-3 and HP-360 detectors positioned at the front center of the phantom. The SPA-3 measurements were performed using the high energy region for the 1.274 MeV  $^{22}\text{Na}$

---

<sup>3</sup> M. W. Mallett, Personal Communication. Feb. 18, 2010.

photon. Since the detectors were not calibrated for this particular geometry the results are reported only as the net count rate (Table 5).

**Table 4.** Fluence and Dose Results.

Run	Location	Energy	Fluence (n cm <sup>-2</sup> )	% Total Fluence	D <sub>HP</sub> (Gy)	D <sub>n,γ</sub> (Gy)	Total D <sub>n</sub> (Gy)	TLD D <sub>n</sub> (Gy)	TLD D <sub>γ</sub> (Gy)
1	2 m Phantom-Front	<0.6 eV	1.9E+11	29	0.11	0.74			
		0.6 eV – 1.1 MeV	3.6E+11	56	2.5	0.92			
		1.1 - 3.3 MeV	6.5E+10	10	2.2	0.09			
		> 3.3 MeV	3.2E+10	5	1.7	0.03			
		<b>Total</b>	<b>6.5E+11</b>		<b>6.5</b>	<b>1.8</b>	<b>8.3</b>		
	4 m Phantom-Front	<0.6 eV	6.3E+10	24	0.04	0.25			
		0.6 eV – 1.1 MeV	1.6E+11	61	1.1	0.42			
		1.1 - 3.3 MeV	3.2E+10	12	1.1	0.04			
		> 3.3 MeV	8.2E+09	3	0.43	0.01			
		<b>Total</b>	<b>2.7E+11</b>		<b>2.7</b>	<b>0.7</b>	<b>3.4</b>		
2	2 m Phantom-Front	<0.6 eV	7.5E+10	33	0.04	0.29			
		0.6 eV – 1.1 MeV	1.0E+11	45	0.72	0.26			
		1.1 - 3.3 MeV	1.7E+10	7	0.56	0.02			
		> 3.3 MeV	3.4E+10	15	1.78	0.04			
		<b>Total</b>	<b>2.3E+11</b>		<b>3.1</b>	<b>0.62</b>	<b>3.7</b>		
	2 m Phantom-Back	<0.6 eV	1.6E+10	12	0.01	0.06			
		0.6 eV – 1.1 MeV	1.1E+11	82	0.78	0.29			
		1.1 - 3.3 MeV	4.7E+09	4	0.16	0.01			
		> 3.3 MeV	3.3E+09	2	0.17	0.00			
		<b>Total</b>	<b>1.4E+11</b>		<b>1.1</b>	<b>0.36</b>	<b>1.5</b>		
3	6 m Phantom-Front	<0.6 eV	5.5E+10	38	0.03	0.22			
		0.6 eV – 1.1 MeV	6.6E+10	46	0.46	0.17			
		1.1 - 3.3 MeV	1.3E+10	9	0.42	0.02			
		> 3.3 MeV	1.1E+10	7	0.56	0.01			
		<b>Total</b>	<b>1.4E+11</b>		<b>1.5</b>	<b>0.41</b>	<b>1.9</b>		
	6 m FIA	<0.6 eV	3.5E+10	29	0.02	0.14			
		0.6 eV – 1.1 MeV	5.7E+10	47	0.39	0.15			
		1.1 - 3.3 MeV	1.7E+10	14	0.57	0.02			
		> 3.3 MeV	1.2E+10	10	0.62	0.01			
		<b>Total</b>	<b>1.2E+11</b>		<b>1.6</b>	<b>0.32</b>	<b>1.9</b>		

**Table 5.** NaCl Phantom Measurement Results.

Run	Location	Time after Exposure (h)	SPA-3 (cpm)	HP-360 (cpm)
1	4 m	3.8	6.86E+04	2.66E+04
		51.2	6.30E+03	2.80E+03
3	6 m	3.2	6.12E+04	2.51E+04

**Conclusions**

The results of the measurements performed for this exercise showed that there is no significant difference in the response between the new PNDs, manufactured by ShieldWerx, and ones previously issued by LANL. The

variability in the results for the old PNDs appears to be greater, likely due to deterioration of the indium foils over time. For the greatest accuracy it is important that the actual foil mass is taken into account; however, use of the average mass is adequate for initial screening and calculations. One main difference between the PNDs was that the plastic used to encase the new dosimeters was much more flexible. This makes it difficult to open the dosimeters without breaking apart the sulfur tablet. Also, in a few cases the adhesive had stuck the bare indium foil to the case making it difficult to extract without tearing.

Comparison of the measurement results between the LANL equipment and LLNLs HPGe detector were favorable for the high energy photon region, but were not as good for the lower energy region. This was later traced to the use of the  $^{137}\text{Cs}$  662 keV photon for establishment of the region and the efficiency calibration. When the detector was re-calibrated using the 511 keV photon from  $^{22}\text{Na}$  the results improved; however LLNLs results were consistently lower than ours. This is likely due to the incomplete annihilation of the  $^{64}\text{Cu}$  positron in the LLNL counting geometry. The availability of spectroscopy capabilities, instead of relying on counts in a region, would improve sample throughput and more rapid determination of the dose by reducing the need to count the indium foils twice to assess the  $^{115\text{m}}\text{In}$  and  $^{116\text{m}}\text{In}$  activities. There were significant differences in the beta activity results between the measurements performed using the HP-360 GM detector and the gas flow proportional and HPGe counters. The cause has not been determined at this time.

Comparisons of the heavy-particle dose, as measured using the PNDs, and the photon doses, measured with the 8823 TLD badge to the values reported by CEA Valduc are shown in Table 6. The heavy-particle neutron doses measured using the PNDs were within  $\pm 7\%$  of the reported delivered doses except for the dosimeters for Run 1 at 4 meters and Run 2 on the back of the phantom. In the second case this was to be expected due to thermalization of the neutrons as they pass through the phantom and a greater relative contribution from in-scatter from other objects in the chamber. The discrepancy in the former is not as easily explained. One possibility is that there is a shift in the neutron energy distribution between the 2 meter and 4 meter positions. Recalculation of the results assuming either a greater proportion of the fluence in the epithermal region or assuming a bare spectrum results in a decrease in the relative bias to approximately 15%.

**Table 6.** Comparison of measured to delivered doses.

Run	Location	LANL		VALDUC		Relative Bias	
		D <sub>HP</sub> (Gy)	D <sub>γ</sub> (Gy)	D <sub>HP</sub> (Gy)	D <sub>γ</sub> (Gy)	D <sub>HP</sub> (%)	D <sub>γ</sub> (%)
1	2 m Phantom-Front	6.5	4.2	6.9	0.5	-5.8	740
	4 m Phantom-Front	2.7	1.6	1.9	0.3	42.1	433
2	2 m Phantom-Front	3.1	4.2	3.2	3.8	-3.1	10.5
	2 m Phantom-Back	1.1	1.6	3.2	3.8	-65.6	-57.9
3	6 m Phantom-Front	1.5	1.8	1.5	2.1	0.0	-14.3
	6 m FIA	1.6	1.5	1.5	2.1	6.7	-28.6

The relative bias in the photon doses, as measured using the 8823 TLD badge, were between -29% to +11% except for both positions for Run 1 and for the Run 2 dosimeters placed on the back of the phantom. Similar to the PND results the latter is to be expected due to attenuation of the incident photons as they pass through the phantom. A more detailed analysis was necessary to explain the results for Run 1. The 8823 dosimeter algorithm calculates the deep dose based on the average of the readings for elements 1 and 7. Element one consists of TLD-700 material (LiF:Mg,Ti enriched in  $^7\text{Li}$ ) under  $600\text{ mg cm}^{-2}$  ABS plastic (Hoffman and Mallett, 1999). Element 7 is the same as element 1 except that it is in a cadmium box with a window facing the front of the dosimeter. For pure photon fields the results for these two elements would be expected to be the same. In the case of these measurements the results for element 7 were greater than those for element 1. This is believed to be the result of the activation of the cadmium by the high neutron fluence and subsequently it being

allowed to decay to background over a period of several weeks with the TLD cards still in place. This would preferentially increase the dose to element 7 over that of element 1. Since the total photon dose for Run 1 was much lower than that for the other runs, the relative contribution from the cadmium activation was much greater. Another interesting factor to note was the ratio of elements 4 to 1. Element 4 is  $\text{CaF}_2:\text{Mn}$  (TLD-400) material under the same filtration as element 1. This ratio is used to estimate the photon energy and is normally expected to be greater than unity for all photon energies. In the case of these measurements the ratios were less than one for all exposures. This is the result of a slightly greater neutron response for the TLD-700 material over that for TLD-400 (Henaish, et. al., 1980). In fact, the ratios observed in these measurements (0.4 to 0.8) were consistent with those found in Henaish, et. al. 1980 (0.44).

One factor that should be addressed before the next exercise is the time required to analyze the PND elements and arrive at an estimate of the dose. The Criticality Dosimetry standard (ANSI, 1969) calls for the determination of the dose within 24 hours of the event. Due to the need to count the indium elements over two days and the data reduction methods this was not achieved. Potential improvements in the process would be: 1) the use of detectors capable of resolving the  $^{115\text{m}}\text{In}$  and  $^{116\text{m}}\text{In}$  photons, allowing their assessment using a single count; 2) investigation of the potential use of just the indium data for a preliminary assessment of the total dose; and 3) development of a form based application that would guide the user in data input and processing. In the case of a criticality accident at LANL, the elements would be analyzed using HPGe detectors, which would address the first item. However, it would be advantageous to have similar capabilities for performing analyses at other locations. A first estimate of the total dose based only on the indium results may be achievable using spectrum specific cross sections and fluence-to-dose conversion factors based on the entire energy range, instead of the limited ranges used during this exercise. A form based application would be helpful in guiding the analyst in the input of data and reduce the potential for human error.

Based on the measurements performed on the sodium phantoms, field instrumentation can be effective in the screening of individuals exposed at neutron doses delivered during this exercise and potentially down to the 1 Gy region. Additionally, screening of the TLDs with the SPA-3 and HP-360 probes showed there was easily measureable activation of components in the badge. Direct measurements of the TLDs could be used to screen exposed individuals. However, this activation may also influence the photon dose estimates by continuing to expose the TLD elements after the event. In future scenarios it would be desirable to separate the TLD element cards from the holders as soon as possible after the end of the exposure.

## References

American National Standards Institute (ANSI). Criticality Dosimetry. ANSI N13.3. 1969.

Asselineau, B.; Trompier, F.; Texier, C.; Itié, C.; M, C.; Médioni, R.; Tikunov, D.; Muller, H.; Pelcot, G. Reference Dosimetry Measurements for the International Intercomparison of Criticality Accident Dosimetry SILENE 9-21 June 2002. Rad. Prot. Dosimetry. 110 Issue 1-4. 2004.

Devine, R.T.; Vigil, M.M.; Martinez, W.A. Using Operational Equipment to Read Accident Dosimeters. Rad. Prot. Dosim. 110 Issue 1-4. 2004.

Devine, R.T. Computation of Cross Sections and Dose Conversion Factors for Criticality Accident Dosimetry. Rad. Prot. Dosim. 110 Issue 1-4. 2004.

Henaish, B.A.; Sayed, A.M.; Morsy, S.M. Fast and Thermal Neutron Response of  $\text{BeO}$  and  $\text{Li}_2\text{B}_4\text{O}_7:\text{Mn}$  in Comparison with  $\text{LiF}$  and  $\text{CaF}_2$ . Nuclear Instruments and Methods. 178: 395-399. 1980.

Hoffman, J.M.; Mallett, M.W. The LANL Model 8823 Whole-Body TLD and Associated Dose Algorithm. Health Phys. 77: S96-S103. 1999.

International Atomic Energy Agency (IAEA). Compendium of Neutron Spectra and Detector Responses for Radiation Protection Purposes. Technical Report Series No. 403. IAEA. Vienna. 2001.

Los Alamos National Laboratory (LANL). The Los Alamos Personnel and Area Criticality Dosimeter Systems: Technical Basis Document. RP2-HPAL-TBD-01. 2006.

**Appendix A**  
PND Element Specific Activities

Run	Location	Element/Isotope	Specific Activity (Bq g <sup>-1</sup> )	Uncertainty (Bq g <sup>-1</sup> )
1	2 m Phantom-Front	Bare In/ <sup>116</sup> In	3.51E+07	4.37E+06
		Cd Covered In/ <sup>116</sup> In	8.97E+06	4.36E+05
		Cd Covered In/ <sup>115m</sup> In	5.95E+03	8.19E+02
		Cd Covered Cu/ <sup>64</sup> Cu	9.48E+03	5.38E+02
		Sulfur/ <sup>32</sup> P	1.39E+02	9.26E+00
	4 m Phantom-Front	Bare In/ <sup>116</sup> In	1.16E+07	4.32E+06
		Cd Covered In/ <sup>116</sup> In	2.97E+06	3.23E+05
		Cd Covered In/ <sup>115m</sup> In	2.45E+03	6.18E+02
		Cd Covered Cu/ <sup>64</sup> Cu	4.21E+03	6.10E+02
		Sulfur/ <sup>32</sup> P	3.51E+01	3.38E+00
2	2 m Phantom-Front	Bare In/ <sup>116</sup> In	1.39E+07	2.49E+06
		Cd Covered In/ <sup>116</sup> In	3.58E+06	6.29E+05
		Cd Covered In/ <sup>115m</sup> In	3.35E+03	6.86E+02
		Cd Covered Cu/ <sup>64</sup> Cu	4.56E+03	8.13E+02
		Sulfur/ <sup>32</sup> P	1.19E+02	7.32E+00
	2 m Phantom-Back	Bare In/ <sup>116</sup> In	2.89E+06	1.20E+05
		Cd Covered In/ <sup>116</sup> In	6.82E+05	7.79E+04
		Cd Covered In/ <sup>115m</sup> In	5.20E+02	9.62E+01
		Cd Covered Cu/ <sup>64</sup> Cu	3.56E+03	7.04E+02
		Sulfur/ <sup>32</sup> P	1.13E+01	1.77E+00
3	6 m Phantom-Front	Bare In/ <sup>116</sup> In	9.83E+06	6.20E+05
		Cd Covered In/ <sup>116</sup> In	2.23E+06	3.63E+05
		Cd Covered In/ <sup>115m</sup> In	1.54E+03	2.08E+02
		Cd Covered Cu/ <sup>64</sup> Cu	2.64E+03	1.16E+03
		Sulfur/ <sup>32</sup> P	3.75E+01	2.03E+00
	6 m FIA	Bare In/ <sup>116</sup> In	6.74E+06	3.12E+05
		Cd Covered In/ <sup>116</sup> In	1.96E+06	5.37E+04
		Cd Covered In/ <sup>115m</sup> In	1.90E+03	7.22E+02
		Cd Covered Cu/ <sup>64</sup> Cu	2.53E+03	7.08E+02
		Sulfur/ <sup>32</sup> P	4.12E+01	1.42E+00